



AQUIFER CHEMISTRY AND MINERAL SATURATION IN SELECTED HIGH TEMPERATURE GEOTHERMAL AREAS

Gültekin Tarcan

Dokuz Eylül University,
Engineering Faculty, Geological Engineering Deptm.,
35100 Bornova, Izmir,
TURKEY
gultekin.tarcan@deu.edu.tr

ABSTRACT

Aquifer fluid compositions have been assessed from analytical data on water and steam samples collected at the wellhead from 28 production wells in eight geothermal areas from five countries (Hveragerdi, Krafla, Námafjall, and Nesjavellir in Iceland; Kizildere in Turkey; Momotombo in Nicaragua; Olkaria in Kenya and Zunil in Guatemala). The state of mineral saturation of the aquifer water with respect to the following minerals was studied: anhydrite, calcite, clinocllore-daphnite, clinozoisite-epidote, grossular, low-albite, microcline (the stable K-feldspar at low temperatures), prehnite, pyrite, pyrrhotite, quartz, wairakite and wollastonite. The aquifer water is close to equilibrium with calcite, quartz, low-albite and microcline. Most of the water is relatively close to wollastonite saturation. The same applies to clinozoisite, prehnite and wairakite although the scatter of the data points is larger than for the previously listed minerals. The waters are saturated or undersaturated with respect to anhydrite and grossular. Oversaturation is indicated for the clinocllore component of chlorite and the epidote component of the epidote solid solution. In the first instance this may be the consequence of the activity of the clinocllore component in the chlorite, but in the latter case faulty thermodynamic data on epidote. The results for all ferrous bearing minerals (daphnite, pyrite and pyrrhotite) indicate undersaturation that increases with increasing temperature. This is most likely an artifact due to faulty data on Fe-ion hydrolysis constants. The results indicate the Kizildere aquifer water is strongly undersaturated with respect to all Ca-bearing minerals. The cause of this apparent undersaturation is precipitation of calcite from the water as it boils, causing wellhead samples to be lower in Ca than the aquifer water.

Assessment of calcite and amorphous silica scaling tendencies for selected well waters indicates that waste fluid disposal at Kizildere is most feasible at the lowest possible temperature if scaling is to be minimized or avoided. Similarly, injection temperatures of about 150 and 200°C are optimal for Zunil and Nesjavellir, respectively.

1. INTRODUCTION

The composition of aquifer fluids in high-temperature geothermal systems is derived from data on the composition of water and steam samples collected at the wellhead and a particular model, which relates the wellhead sample and aquifer fluid compositions. Many studies indicate that geothermal water compositions are controlled by a close approach to mineral-solution equilibria with respect to various elements (Arnórsson et al., 1983a, b; Giggenbach, 1980, 1981, 1988; Michard, 1991; Tole et al., 1993; Gunnarsson and Arnórsson, 1999; Gökğöz, 1998; Arnórsson, 1999, 2000a, b; Stefánsson et al., 2000; Stefánsson and Arnórsson, 2000; Karingithi, 2000; Gudmundsson and Arnórsson, 2001; Palandri and Reed, 2001). Changes which occur in temperature and water composition during boiling between aquifer and wellhead, generally lead to changes in mineral saturation. Such changes may result in mineral precipitation or mineral dissolution. Together with physical processes in the depressurization zone around wells, these changes may cause well discharge compositions to differ from the chemical composition of the aquifer fluid.

The purpose of the present study is to examine the state of mineral saturation in the aquifer of selected liquid-dominated high-temperature geothermal systems occurring in different geological environments. The systems considered include four from Iceland (Hveragerdi, Krafla, Námafjall and Nesjavellir), Kizildere in Turkey, Olkaria in Kenya, Momotombo in Nicaragua and Zunil in Guatemala. All these systems occur in volcanic rocks, ranging from basaltic to silicic in composition except for Kizildere, which is hosted in metamorphic and sedimentary rocks. Table 1 gives the chemical composition of the well discharges for the selected wells. All the waters are relatively dilute. The aquifer temperatures range from 195 to 305°C. The majority of the wells have excess enthalpy, yet some have liquid enthalpy.

Figure 1 shows the locations of the selected geothermal areas. The geological characteristics of the areas selected for the present study and their development and exploitation histories have been described by various authors: Kizildere by Simsek (1985); Olkaria by Arnórsson et al. (1990), Omenda (1998), Muchemi (1999), Karingithi (2000); Zunil by Arnórsson (1995), Labota and Palma (2000) and Momotombo by Combredet et al. (1987) and Arnórsson (1997). The Krafla and Námafjall areas have been described by Ármannsson et al. (1987, 1989), Nielsen et al. (2000), Gudmundsson and Arnórsson (2001), and finally Hveragerdi and Nesjavellir by Franzson (2000).

2. SAMPLE COLLECTION

All the samples from the Icelandic wells considered in this study were collected at elevated pressure with the aid of a Webre separator connected to a two-phase pipeline close to each wellhead (see Gudmundsson and Arnórsson, 2001). Steam samples from Olkaria were collected under pressure from separators by each wellhead, but water samples from weirboxes (Karingithi, 2000). Thus, a fraction of the discharge was not sampled, i.e. the steam formed by flashing of the separated water during pressure drop from the wellhead separator to atmospheric pressure. The Kizildere, Momotombo and Zunil wells were sampled in the same way (Arnórsson, 1995, 1997; Lindal and Kristmannsdóttir, 1989, Gökğöz, 1998; ENEL, 1989; Giese, 1997).

The data input for the WATCH program from wet-steam wells needed to calculate aquifer fluid compositions require that both water and steam samples be collected at the same pressure. In order to make the primary data conform to the requirements of the WATCH program, gas concentrations in steam samples were corrected by adding the steam that escapes from the atmospheric silencer to the steam sampled, assuming the former to be gas free.

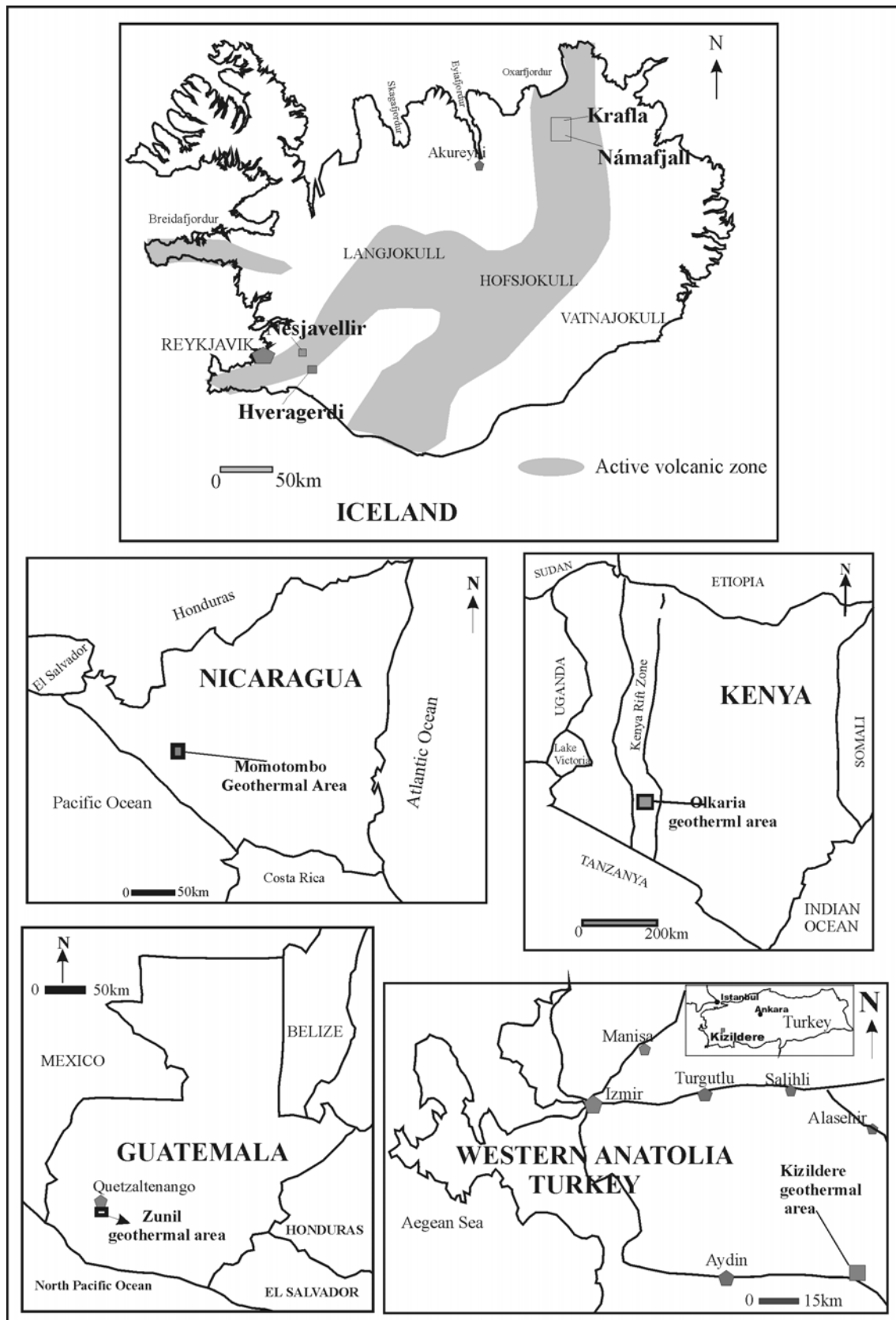


FIGURE 1: Locations of the selected high-temperature areas for the present study

TABLE 1: Chemical analyses of the water and steam samples from the high-temperature wells selected for this study; concentrations are in mg/kg and mmol/kg for water and steam samples, respectively, unless otherwise stated

No	Location	Well/Aquifer ^k	Temp. (°C)	Sampl. pressure (bar-g)	Enthalpy (kJ/kg)	Water sample														Steam Sample						
						CO ₂	H ₂ S	NH ₃	B	SiO ₂	Na	K	Mg	Ca	F	Cl	SO ₄	Al	Fe	pH/°C	CO ₂	H ₂ S	H ₂	O ₂	CH ₄	N ₂
1 ^a	Momotombo	MT-23	229 ^a	5.45 ⁱ	1095	26.2	1.6	1.0	27.1	437	1619.0	212.7	0.160	52.1	2954	89.2	0.21	0.730	7.39/25	47.6	1.27	0.10	0.000	0.07	2.13	
2 ^a	Momotombo	MT-26	238 ^a	5.50 ⁱ	1008	6.7	1.5	0.9	32.1	541	1886.0	268.7	0.100	57.8	3475	89.3	0.23	0.030	8.34/25	27.5	1.02	0.04	0.000	0.02	0.92	
3 ^b	Hvergerdi	W-7	225	12.00	967	43.4	23.4	0.0	1.0	425	176.8	21.3	0.008	1.7	0.6	186	35.2	0.005	8.86/20	69.8	6.05	4.78	0.000	0.56	74.96	
4 ^c	Krafla	K-9	215	8.40	1063	57.6	57.6	0.5	519	221.6	26.2	0.003	3.2	0.9	23	307.4	1.12	0.003	9.42/25	53.0	5.1		0.000	0.21	1.87	
5 ^c	Námafjall	N-4	240	5.10	1035	3.5	10.6	0.9	522	164.1	19.9	0.003	4.4	0.7	31	47.1	0.65	0.006	9.59/22	70.0	26.3	36.40	0.017	3.61	2.51	
6 ^d	Kizildere	KD-6	196	4.02 ⁱ	834	1695.0	0.7	20.0	310	1134.0	131.0	0.273	1.2	17.3	46	643.5	0.15	0.000	7.76/23	90.8 ^m	<0.1 ^m	0.10 ^m	1.630 ^m	0.10 ^m	7.37 ^m	64.9
7 ^d	Kizildere	KD-16	211	3.91 ⁱ	902	1854.0	1.3	27.0	393	1245.0	151.0	0.291	3.7	23.8	49	656.0	0.30	0.025	8.12/22	88.4 ^m	<0.1 ^m	<0.10 ^m	2.400 ^m	<0.10 ^m	9.20 ^m	53.5
8 ^e	Kizildere	KD-13	195	3.86 ⁱ	830	1391.0		305	1214.0	132.0	0.180	0.4	17.2	100	337.0	0.55	<0.10	9.63/25	206.1	0	0.05	0.005	1.35	1.29		
9 ^e	Kizildere	KD-22	202	3.80 ⁱ	861	1417.0		316	1282.0	144.0	0.150	0.5	18.5	100	504.0	0.55		9.12/25	97.5 ^m	<0.1 ^m	<0.10 ^m	0.600 ^m	0.10 ^m	1.70 ^m	47.2	
10 ^f	Nesjavellir	NG-6	300	14.60	1790	32.1	63.0	822	134.0	28.8	0.003	0.2	0.9	119	3.8	1.92	0.014	8.14/21	216.0	64.8	49.90	0.382	0.02			
11 ^f	Nesjavellir	NJ-11	305	14.60	1510	27.7	83.7	880	132.0	27.2	0.002	0.3	1.1	80	12.9	2.82	0.066	8.88/21	195.0	81.5	85.50	0.181	1.14			
12 ^f	Nesjavellir	NJ-13	300	15.40	1880	21.4	65.9	907	130.0	29.7	0.000	0.1	1.0	111	2.4	2.12	0.019	8.42/21	154.0	34	27.90	0.059	0.14			
13 ^f	Nesjavellir	NJ-16	285	14.40	1810	33.8	113.0	785	135.0	26.8	0.005	0.9	1.2	60	26.3	2.24	0.015	8.87/21	144.0	14.7	17.50	0.077	0.15			
14 ^c	Krafla	K-12	275	13.30	1831	76.0	63.6	1.7	759	135.4	26.2	0.039	2.4	1.6	35	74.9	1.48	0.142	6.98/20	314.0	27.3	13.30	0.031	0.35	1.31	
15 ^c	Krafla	K-30	291 ^h	28.50	1712	102.5	94.0	2.7	765	139.3	34.0	0.000	0.8	1.2	50	45.2	1.19	0.013	6.84/20	491.0	52.2	13.10	0.047	0.02	3.72	
16 ^c	Námafjall	N-11	260	25.30	1850	3.5	97.8	2.3	546	100.5	15.6	0.003	0.4	0.8	29	20.2	1.65	0.032	8.35/21	110.0	42.7	54.80	0.003	0.62	2.07	
17 ^c	Krafla	K-17	275	21.70	1881	47.1	98.1	1.5	643	112.4	20.3	0.003	0.0	2.0	18	92.2	1.14	0.012	8.89/24	184.0	26.4	29.70	0.000	0.80	2.14	
18 ^c	Momotombo	MT-02	225 ^h	5.55 ⁱ	2238	34.3	0.9	0.5	20.9	406	1210.0	156.9	0.100	23.3	1738	210.2	0.27	0.030	8.65/25	365.1	7.5	0.00	0.000	0.00	0.00	
19 ^c	Momotombo	MT-35	269 ^h	5.55 ⁱ	1654	10.6	1.9	0.5	32.0	864	1838.0	342.6	0.070	16.4	3128	46.7	0.14	0.030	8.77/25	268.2	4.35	0.21	0.000	0.84	13.16	
20 ^d	Zunil	ZCQ-3	265	7.30	1423	51.2		33.0	741	860.0	175.4	0.190	10.8	3.6	1377	27.0	1.09	0.060	8.04/25	94.6 ^m	4.07 ^m	0.17 ^m	0.004 ^m	0.012 ^m	0.98 ^m	3.3
21 ^d	Zunil	ZCQ-4	249	5.80	2427	31.7		29.5	574	884.0	141.0	0.370	29.0	1490	56.0	1.02	0.480	7.95/25	94.4 ^m	4.60 ^m	0.43 ^m	0.002 ^m		0.99 ^m	2.0	
22 ^d	Zunil	ZCQ-5	255	7.51	2218	30.3		59.2	524	1150.0	201.0	0.290	26.9	6.0	1760	30.0	1.81	1.820	7.76/25	96.5 ^m	2.14 ^m	0.21 ^m	0.003 ^m	0.012 ^m	0.97 ^m	3.5
23 ^d	Zunil	ZCQ-6	290	6.73	2343	101.7		37.0	737	892.0	170.0	0.530	7.4	35.0	1447	38.0	0.87	0.030	8.36/25	97.5 ^m	1.70 ^m	0.06 ^m	0.001 ^m	0.60 ^m		4.5
24 ^g	Olkaria	OW-10	245	4.53 ⁱ	2535	114.2	0.9	8.0	638	855.1	129.7	0.176	3.9	81.1	1080	57.0	0.99	0.099	8.75/25	75.8	4.20	3.56	0.700	0.60	3.33	
25 ^g	Olkaria	OW-16	240	4.66 ⁱ	1384	82.9	2.1	5.4	573	481.5	69.0	0.047	1.0	69.6	636	35.9	0.69	<0.02	8.97/25	51.4	5.17	2.62	0.005	0.20	1.34	
26 ^g	Olkaria	OW-25	260	4.90 ⁱ	2516	149.6	2.1	5.5	641	522.0	94.5	0.106	1.2	70.1	671	28.4	0.51	<0.02	9.15/25	75.0	5.37	4.15	0.027	0.16	2.35	
27 ^g	Olkaria	OW-901	250	1.56 ⁱ	1854	565.6	18.3	2.4	529	505.8	56.5	0.029	0.7	80.1	280	123.8	0.68	0.028	9.80/25	182.6	4.85	2.37	0.110	0.30	5.05	
28 ^g	Olkaria	OW-902	220	1.01 ⁱ	1108	433.8	2.0	1.5	477	447.8	41.4	0.049	1.3	51.5	212	99.9	2.12	0.083	9.55/25	178.7	0.47	0.04	0.350	0.77	13.55	

Data taken from ^aArnórsson, 1997; ^bArnórsson and Gunnlaugsson, 1985; ^cGudmundsson and Arnórsson, 2001; ^dJindal and Kristmannsdóttir, 1989; ^eGiese, 1997; steam analyses for the wells KD-6, 13, 16-22 were taken from ENEL, 1989; ^fReykjavík Energy-Iceland (2000) unpublished data, ^gKarínghí, 2000, ^hNa/K geothermometry temperature. ⁱWater samples were collected from the weirbox. For these samples gas concentrations in steam have been modified. They correspond to concentrations in steam at 1 bar-a. ^jDerived assuming liquid enthalpy, ^kMeasured aquifer temperature unless otherwise specified, ^lMeasured water phase pH at temperature °C, ^mValues of steam samples are % by volume

3. ASSESSMENT OF AQUIFER FLUID COMPOSITIONS FROM WET-STEAM WELL DATA

In order to calculate the chemical composition of the total discharge of wet-steam wells it is necessary to collect samples of both water and steam at a measured separation pressure and calculate the water/steam ratio of the discharge from knowledge of well discharge enthalpy. Assessment of aquifer fluid compositions from wet-steam well data is generally more complex. The simplest case occurs when the level of first boiling is within the well. This means that only liquid water exists in the aquifer. Accordingly, the enthalpy of the total well discharge and its composition are the same as those of the water entering the well (Arnórsson, 2000a; Arnórsson et al., 2000). In terms of thermodynamics, the well is regarded as an isolated system (no mass and heat transfer) and the boiling is, therefore, adiabatic. However, such conditions are not always met with, at least when extensive boiling starts in the producing aquifers of wells. Both the discharge enthalpy and the total discharge composition may depart from those of the aquifer fluid. When this is the case, specific models are needed to connect well discharge and aquifer fluid compositions (Arnórsson et al., 1990).

If the fluid discharged can be treated, in thermodynamic terms, as an isolated system, which can be assumed to be valid for wells with liquid enthalpy (the enthalpy of the well discharge is the same as that of liquid water at the aquifer temperature), the total discharge composition equals that of the aquifer water. This treatment may also be valid for excess enthalpy wells, if the excess enthalpy is due to the presence of steam in the aquifer (Arnórsson, 2000a, b). If the fluid cannot be regarded as an isolated system, it may either be closed (heat is not conserved) or open (neither heat nor mass are conserved). In a closed system the enthalpy is not a conserved quantity. Excess enthalpy (the discharge enthalpy is higher than that of liquid water at aquifer temperature) would be produced by conductive heat flow from the aquifer rock to the fluid. Alternately, excess discharge enthalpy could result from segregating the flowing water and steam in the aquifer (an open system) (Arnórsson et al., 1990; Karingithi, 2000). Difficulties in evaluating the relative importance of the processes that lead to excess discharge enthalpy lead to uncertainties in the calculation of the chemical composition of the aquifer fluid from analytical data on water and steam samples collected at the wellhead.

The enthalpy of saturated steam varies with temperature. It reaches maximum around 235°C. It is, however, about constant in the range 180-270°C (equivalent to 10-55 bars-a vapour pressure) but at higher and lower temperatures it falls (Arnórsson et al., 2000). As a result, steam formation by depressurization is little affected by the steam to water ratio of a fluid sensing pressure drop in this range (10-55 bars-a), but at lower and higher pressures, water evaporation by depressurization increases and decreases with increasing steam fraction of the fluid, respectively. In fact depressurization of >270°C fluid may lead to steam condensation.

Most of the wells selected for the present study have excess enthalpy (Table 1). However, some wells have liquid enthalpy (KD-6, KD-16, KD-13 and KD-22 at Kizildere, MT-23 and MT-26 at Momotombo, and W-7, K-9 and N-4 at Hveragerdi, Krafla and Námafjall, respectively). For the liquid enthalpy wells, the aquifer water composition was calculated with the aid of the WATCH speciation program (Arnórsson et al., 1982 and Bjarnason, 1994) on the basis that the enthalpy is equal to that of steam saturated water at the selected aquifer temperature. For the Icelandic excess enthalpy wells, the water and steam compositions were first calculated at 180°C (10 bars-a vapour pressure) using measured discharge enthalpy values. Subsequently, the aquifer water composition was calculated from the calculated compositions at 180°C, taking the fluid enthalpy to be equal to liquid enthalpy at aquifer temperature. This method of calculation of aquifer fluid composition yields results which are consistent with the open system model, i.e. the excess discharge enthalpy is taken to result from phase segregation in the depressurization zone around wells. For other excess enthalpy wells, the aquifer water composition was obtained from water and steam sample compositions at atmospheric pressure, taking the enthalpy to be that of liquid water at aquifer temperature. These wells all have wellhead separators. In this approach, evaporation by a pressure drop upstream from the wellhead separator is underestimated but overestimated downstream from the separator. The errors on the two estimates approximately nullify each other (Karingithi, 2000). Therefore, this calculation procedure yields aquifer water compositions that correspond reasonably with the open system model.

4. SPECIATION CALCULATIONS AND MINERAL SATURATION

Version 2.1A of the WATCH program (Bjarnason, 1994) was used to calculate aqueous speciation distribution in the aquifer water. Reference temperature for the speciation calculations can be chosen in several ways, i.e. measured aquifer temperature, a geothermometry temperature or in fact any arbitrary value. The geothermometry temperatures are retrieved from the activities of the respective chemical species. The thermodynamic database for the calculations is that given by Arnórsson et al. (1982) except for the hydrolysis constants for aluminium and ferric and ferrous iron and gas solubilities, which are from Arnórsson and Andrésdóttir (1999), Diakonov et al. (1999), Arnórsson et al. (2001), and Arnórsson et al. (1996), respectively. The redox potential derived from the H_2S/SO_4 redox couple was used to retrieve the aqueous Fe^{+2}/Fe^{+3} activity ratio and the relative abundance of the ferrous and ferric species. In addition, the Al-Si dimer was considered for the speciation calculations for which Pokrovski et al. (1998) present thermodynamic data. This dimer hosts the majority of the dissolved Al and, therefore, affects significantly retrieved values for activity products of all Al-bearing minerals. The pH in the new version of WATCH is calculated by taking into account all species of major components that can combine with H^+ , whereas only carbonate, sulphide, silica, borate and sulphate species were considered in the original version.

The activity products for these minerals were calculated: Anhydrite, calcite, clinocllore, clinzoisite, daphnite, epidote, grossular, low-albite, microcline (the stable K-feldspar at low temp.), prehnite, pyrite, pyrrhotite, quartz, wairakite and wollastonite. The solubility constants for the same minerals, as a function of temperature, were obtained from Gudmundsson and Arnórsson (2001). Comparing the solubility constant (K) and the activity product (Q) permits evaluation of whether the water is undersaturated ($Q < K$), at equilibrium ($Q = K$) or oversaturated ($Q > K$) with a particular mineral. The minerals considered in this study are those identified as hydrothermal minerals in the Krafla and Námafjall geothermal aquifers.

5. MINERAL SATURATION

The solubility product (Q) of each of the minerals discussed in Section 4 has been plotted against temperature in Figures 2-9. Also shown in the diagrams of these figures are the solubility constant (K) curves for each mineral. Departures from equilibrium for each mineral reaction are given in terms of a saturation index, $\log(Q/K)$, in Table 2, as well as average and mean departures from equilibrium and standard deviation of the mean departure. If average departure from equilibrium is zero, it indicates that, on average, all the aquifer waters considered are just at equilibrium. The mean value, on the other hand, gives the mean departure (absolute value) from equilibrium. Negative $\log(Q/K)$ values in Table 2 indicate undersaturation and positive values oversaturation.

TABLE 2: Reactions and departures from equilibrium for each mineral (with respect to SI values)

Mineral	Reaction*	Average departure	Mean departure	Standard deviation
Anhydrite	$Anh = Ca^{+2} + SO_4^{-2}$	-0.921	0.737	0.861
Calcite	$Cal = Ca^{+2} + CO_3^{-2}$	0.009	0.430	0.546
Clinocllore	$Clc + 10H_2O = 5Mg^{+2} + 2Al(OH)_4^- + 3H_4SiO_4 + 8OH^-$	6.395	3.807	4.769
Clinzoisite	$Czo + 12H_2O = 2Ca^{+2} + 3Al(OH)_4^- + 3H_4SiO_4 + OH^-$	-0.877	1.831	2.334
Daphnite	$Dap + 10H_2O = 5Fe^{+2} + 2Al(OH)_4^- + 3H_4SiO_4 + 8OH^-$	-4.691	4.094	4.948
Epidote	$Epi + 12H_2O = 2Ca^{+2} + Fe(OH)_4^- + 2Al(OH)_4^- + 3H_4SiO_4 + OH^-$	1.774	1.306	1.761
Grossular	$Gro + 4H^+ + 8H_2O = 3Ca^{+2} + 2Al(OH)_4^- + 3H_4SiO_4$	-2.368	2.554	3.483
Low-albite	$Low-alb + 8H_2O = Na^+ + Al(OH)_4^- + 3H_4SiO_4$	-0.247	0.249	0.299
Microcline	$Mic + 8H_2O = Na^+ + Al(OH)_4^- + 3H_4SiO_4$	-0.379	0.254	0.312
Prehnite	$Pre + 10H_2O = 2Ca^{+2} + 2Al(OH)_4^- + 2OH^- + 3H_4SiO_4$	-0.603	1.787	2.341
Pyrite	$Pyr + 2H^+ + H_2 = 2H_2S + Fe^{+2}$	-5.113	0.811	1.048
Pyrrhotite	$Pyrr + 2H^+ = H_2S + Fe^{+2}$	-1.82	0.803	0.941
Quartz	$Qtz = H_4SiO_4$	0.000	0.039	0.050
Wairakite	$Wai + 10H_2O = 2Ca^{+2} + 2Al(OH)_4^- + 4H_4SiO_4$	0.193	0.906	1.135
Wollastonite	$Wol + 2H^+ + H_2O = Ca^{+2} + H_4SiO_4$	-0.819	0.999	1.369

*taken from Gudmundsson and Arnórsson (2001)

5.1 Anhydrite and calcite

The activity product for anhydrite is shown in Figure 2A together with the anhydrite solubility curve. Most of the waters are undersaturated with respect to anhydrite. However, all wells at Momotombo and Zunil are very close to saturation, as well as the relatively cold wells at Námafjall (N-4) and Krafla (wells K-9 and K-12). The average and mean departures from saturation are -0.921 and 0.737 log(Q/K) units, respectively, and the standard deviation of the departure from equilibrium is 0.861 log(Q/K) units. As for calcite discussed below, the Nesjavellir and Kizildere wells show the highest degree of undersaturation. Anhydrite has been identified as a hydrothermal mineral at Kizildere. There is, thus, apparent inconsistency in the results. This is due to loss of calcium from solution through calcite precipitation. Saturation for the Momotombo and Zunil waters is related to higher salinity as compared to other waters considered in this study. Calcium concentrations in geothermal water is positively related to water salinity.

The results shown in Figure 2B indicate that most of the aquifer waters are slightly calcite oversaturated whereas a few are somewhat undersaturated, in particular those from Kizildere and Nesjavellir. The average and mean departure from saturation are 0.009 and 0.430 log(Q/K) units, respectively, and the standard deviation of the departure from equilibrium is 0.546 log(Q/K) units. The strong undersaturation of the Kizildere wells, especially KD-6 and KD-22, is considered to be due to low calcium in the discharged water which is a consequence of calcite precipitation from the flashed water. Probably the same applies to three of the Nesjavellir wells considered.

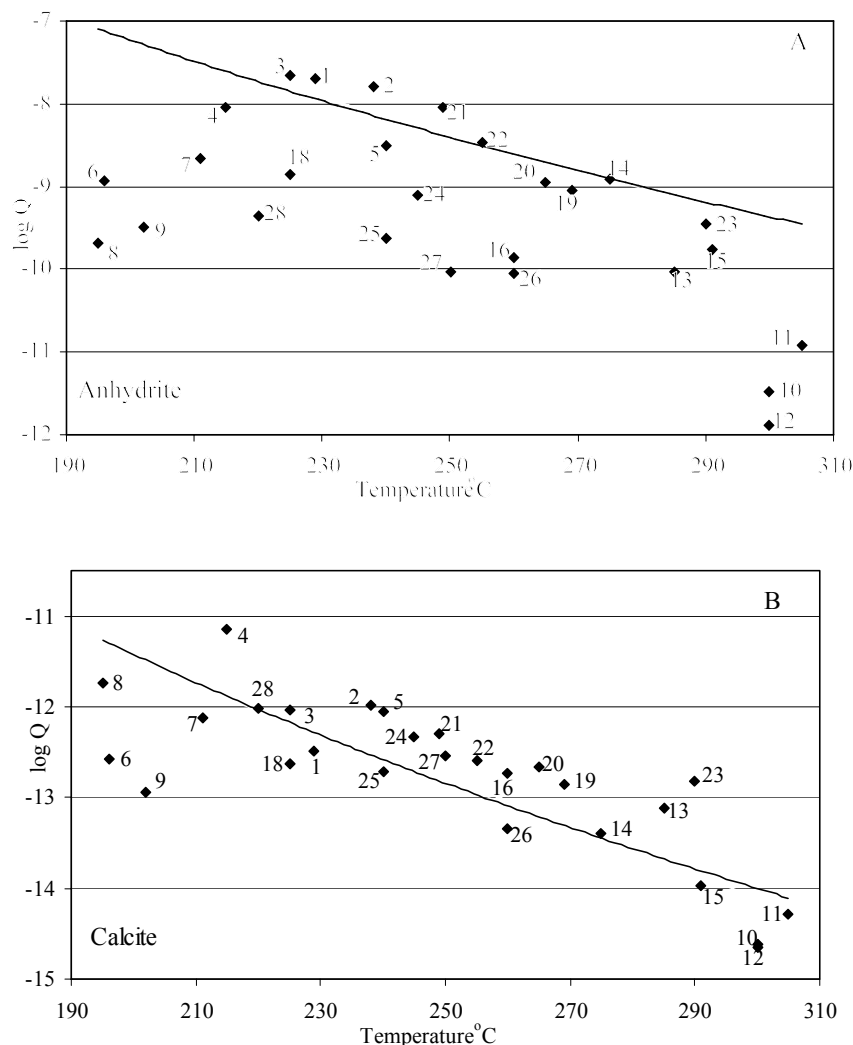


FIGURE 2: The saturation state of aquifer waters in selected geothermal systems with respect to anhydrite and calcite; the solid curves represent the solubility constant values (log K) for each mineral and the numbers refer to the first column of Table 1

Equilibrium with calcite is rapidly attained at high temperatures. For this reason it is to be expected that high-temperature geothermal water would be very close to being calcite saturated. As the solubility of calcite is pH-dependent, one of the main errors involved in calculating calcite saturation in the aquifer of wet-steam wells, from data on the chemical composition of water and steam samples collected at the surface involves, the calculation of the aquifer pH. In view of this and other errors involved in sampling, analysis and assessment of the speciation distribution in the aquifer water, departure in logQ from the calcite solubility constant curve of 0.3 is not regarded as significant (Arnórsson, 1989; Karingithi, 2000). Accordingly, it is concluded that most of the aquifer waters considered for the present study are at equilibrium with calcite within the error of estimation of log(Q/K).

5.2 Clinocllore and daphnite

The solubility products for the clinocllore and daphnite end-members of chlorite show much scatter (Figure 3). Generally, the aquifer waters are oversaturated with respect to clinocllore, up to 15 orders of magnitude. This large departure is related to the complex formula of this mineral. It is below about two orders of magnitude per OH. The average and mean departures are 0.80 and 0.48 log(Q/K) units per OH, respectively, and standard deviation of the mean is 0.60 log(Q/K) units per OH. The results presented in

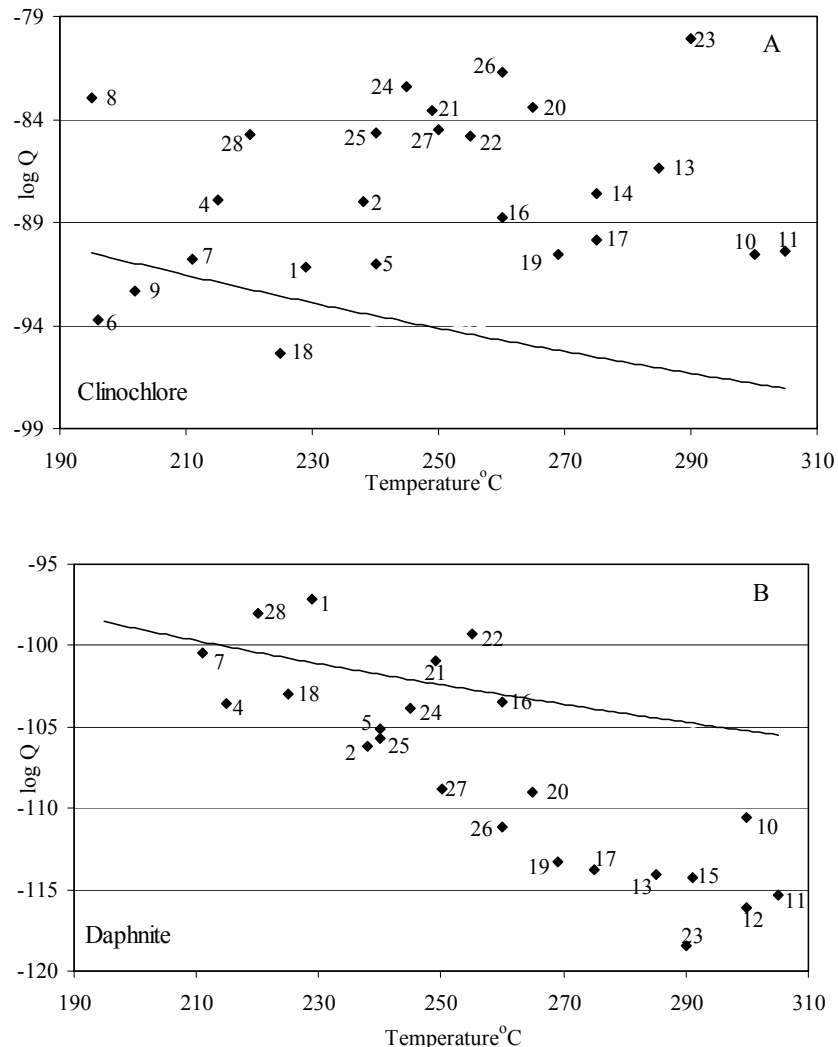


FIGURE 3: The saturation state of aquifer waters in selected geothermal systems with respect to clinocllore and daphnite; the solid curves represent the solubility constant values (log K) for each mineral and the numbers refer to the first column of Table 1

Figure 3 assume the presence of the Al-Si dimer. If this dimer were ignored for the speciation calculations, the degree of clinocllore oversaturation would be somewhat higher. Except for Krafla and Nesjavellir, the composition of the chlorite in the areas considered for present study, i.e. the activity of clinocllore end-member in the chlorite, is not known. Variation in the composition of the chlorite can be expected to affect values by several orders of magnitude and thus influence the scatter of the data points in Figure 3.

Contrary to clinocllore, the aquifer waters are systematically undersaturated with respect to the daphnite component of chlorite. The scatter is even larger and the degree of undersaturation increases with increasing temperature. The average and mean departures from equilibrium are -0.59 and 0.51 log(Q/K) units per OH, respectively. The relationship between logQ and temperature for daphnite is similar to that observed for other Fe-bearing minerals. Faulty values in the calculated activity of the Fe⁺² ion are a likely cause (Arnórsson et al., 2001).

5.3 Clinozoisite and epidote

The solubility product data points for clinozoisite show much scatter (Figure 4A). If the Kizildere data are excluded, they scatter around the solubility curve, the departure being as much as 2.5 log(Q/K) uts.

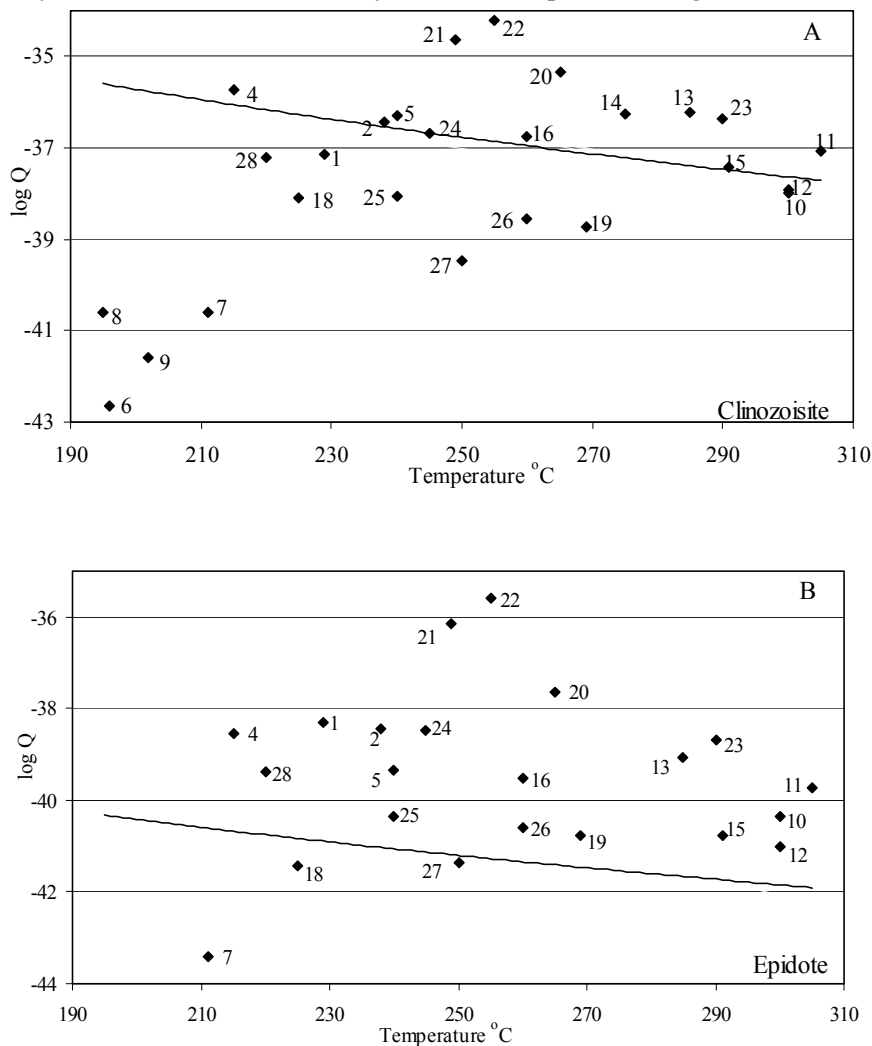


FIGURE 4: The saturation state of aquifer waters in selected geothermal systems with respect to clinozoisite and epidote; the solid curves represent the solubility constant values (log K) for each mineral and the numbers refer to the first column of Table 1

The Kizildere aquifer water is highly undersaturated. The cause is partly low calcium in the well discharge as explained for calcite. Excluding the Kizildere data, the average and mean departures from equilibrium are -0.074 and 1.092 log(Q/K) units, respectively, and the standard deviation is 1.397. The large scatter of the data points is related to the complex composition of clinozoisite in relation to minerals of simpler composition such as calcite. However, variable composition of the epidote in the areas under study is also expected to contribute, i.e. variable activity of the clinozoisite component in the epidote solid solution.

For epidote, the scatter of the data points is similar to that for clinozoisite and the causes are considered to be same. However the aquifer waters are systematically oversaturated (Figure 4B). According to Gudmundsson and Arnórsson (2001), the cause of this apparent oversaturation is probably faulty thermodynamic data on the epidote mineral.

5.4 Grossular and wairakite

These two Ca-Al-silicates show similar scatter on the logQ vs. temperature diagrams (Figure 5). The data points representing the activity products for grossular show rather large scatter (Figure 5A). All the Zunil waters, and two Icelandic waters (K-9 and NJ-16) are slightly oversaturated with respect to grossular. The remainder of the aquifer waters are slightly to somewhat undersaturated. Average and mean departures from equilibrium and the standard deviation of the mean are given in Table 2. High standard deviation is due to the Kizildere waters showing strong undersaturation.

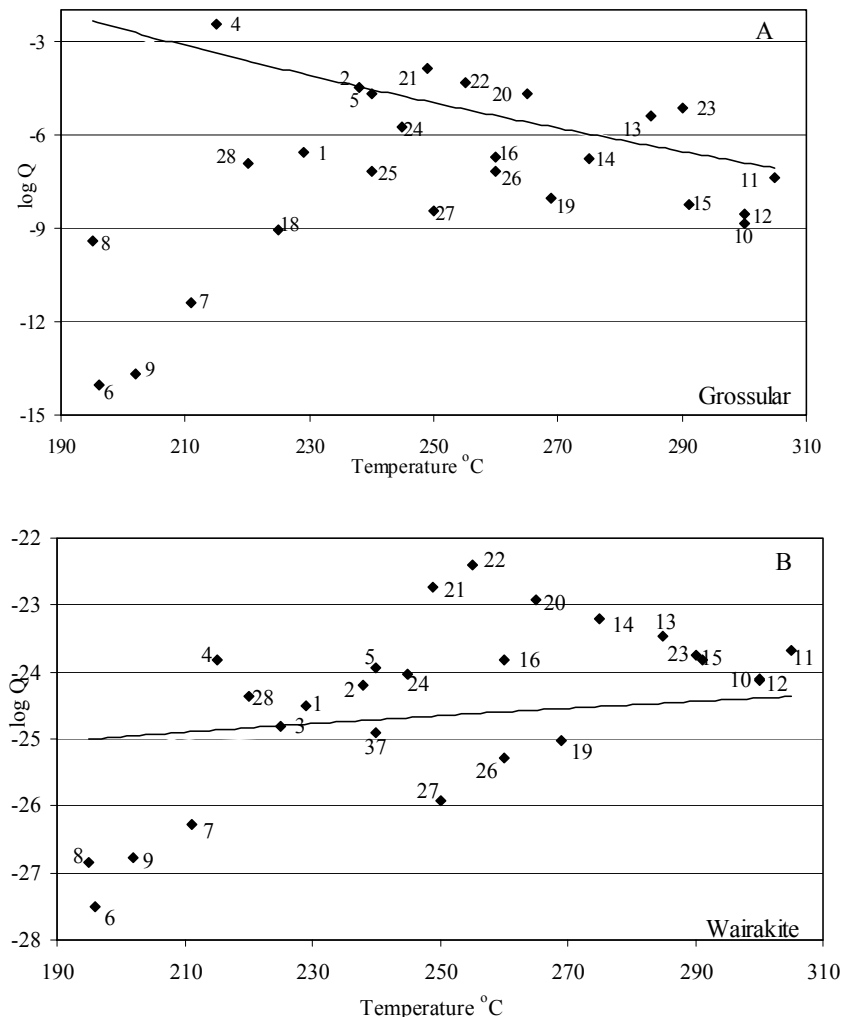


FIGURE 5: The saturation state of aquifer waters in selected geothermal systems with respect to grossular and wairakite; the solid curves represent the solubility constant values (log K) for each mineral and the numbers refer to the first column of Table 1

Most of the samples are relatively close to wairakite saturation, the average and mean departures, excluding the Kizildere waters, are 0.542 and 0.595 log(Q/K) units (Figure 5B). These are not high in view of the stoichiometry of the mineral. The results for the Kizildere wells indicate strong undersaturation, which is not real, being caused by the low calcium content of the water samples. In relation to the aquifer waters, the surface samples are low in Ca due to calcite precipitation during boiling of the ascending aquifer water.

5.5 Low-albite and microcline

The results depicted in Figure 6A for low-albite show slightly negative log(Q/K) values. The average and mean departure from equilibrium corresponds to -0.247 and 0.249 log(Q/K) units, respectively. The picture for microcline (the stable K-feldspar at low temperatures) is practically the same, average and mean departures from equilibrium being -0.379 and 0.254 log(Q/K) units, respectively (Figure 6B).

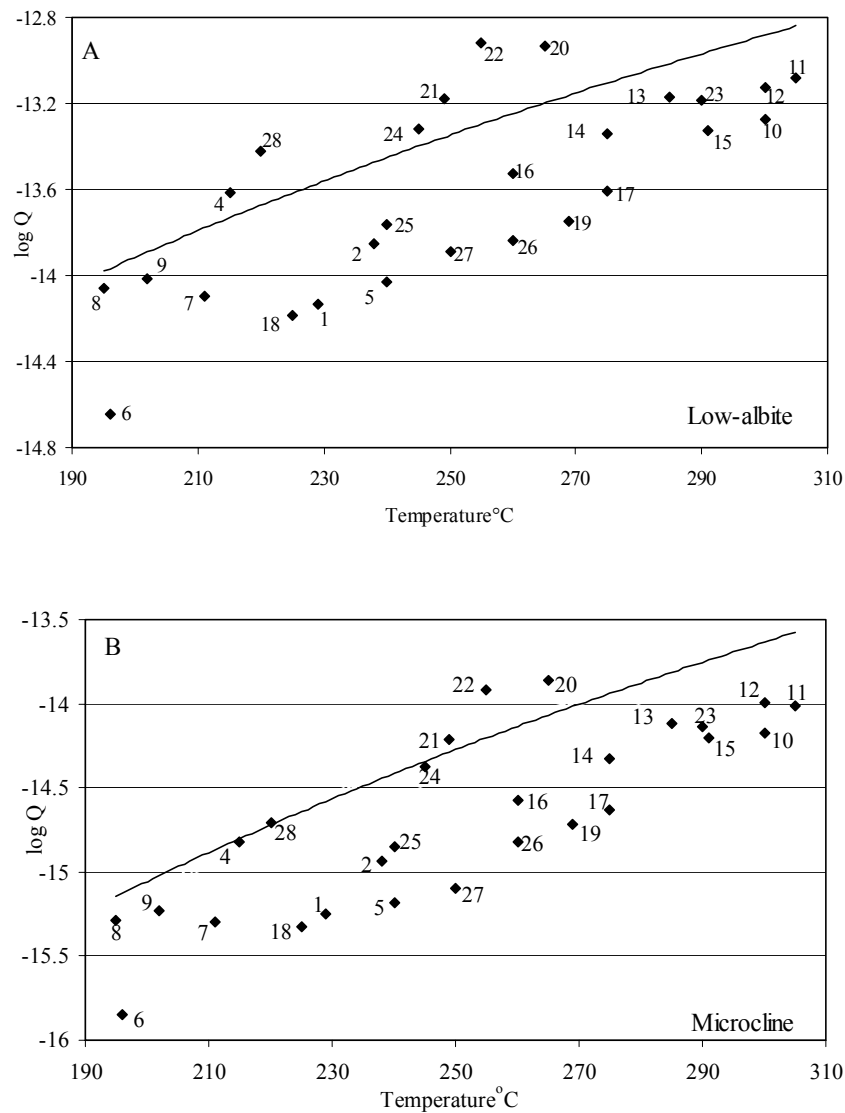


FIGURE 6: The saturation state of aquifer waters in selected geothermal systems with respect to low-albite and microcline; the solid curves represent the solubility constant values (log K) for each mineral and the numbers refer to the first column of Table 1

In calculating aqueous species distribution and, therefore, the solubility products for the alkali feldspars, the Al-Si dimer, for which, Pokrovski et al. (1998) present data, was considered. This dimer constitutes a substantial fraction of the aqueous aluminium in the geothermal waters considered. Had this dimer not been considered, all logQ data points for low-albite and microcline would be shifted by about 0.5 to higher values, i.e. from systematic undersaturation to systematic oversaturation. Stefánsson and Arnórsson (2000) have concluded that the stability of the Al-Si dimer may be overestimated, at least at high temperatures. These results are substantiated by the present study. Average departures of these minerals obtained for this study are very close to Stefánsson's and Arnórsson's (2000) findings. In view of the errors involved in calculating the log(Q/K) values for the alkali feldspars, it is concluded that the aquifer waters considered for the present study are, within error limits, at equilibrium with both low-albite and microcline (the stable K-feldspar at low temperatures). The present results are, thus, consistent with field data which show that low-albite and microcline typically form as secondary minerals in active geothermal systems.

5.6 Pyrite and pyrrhotite

The plot of the activity product for pyrite and pyrrhotite is shown in Figure 7A-B. The results indicate that all the waters are strongly undersaturated with respect to both minerals. These minerals are present

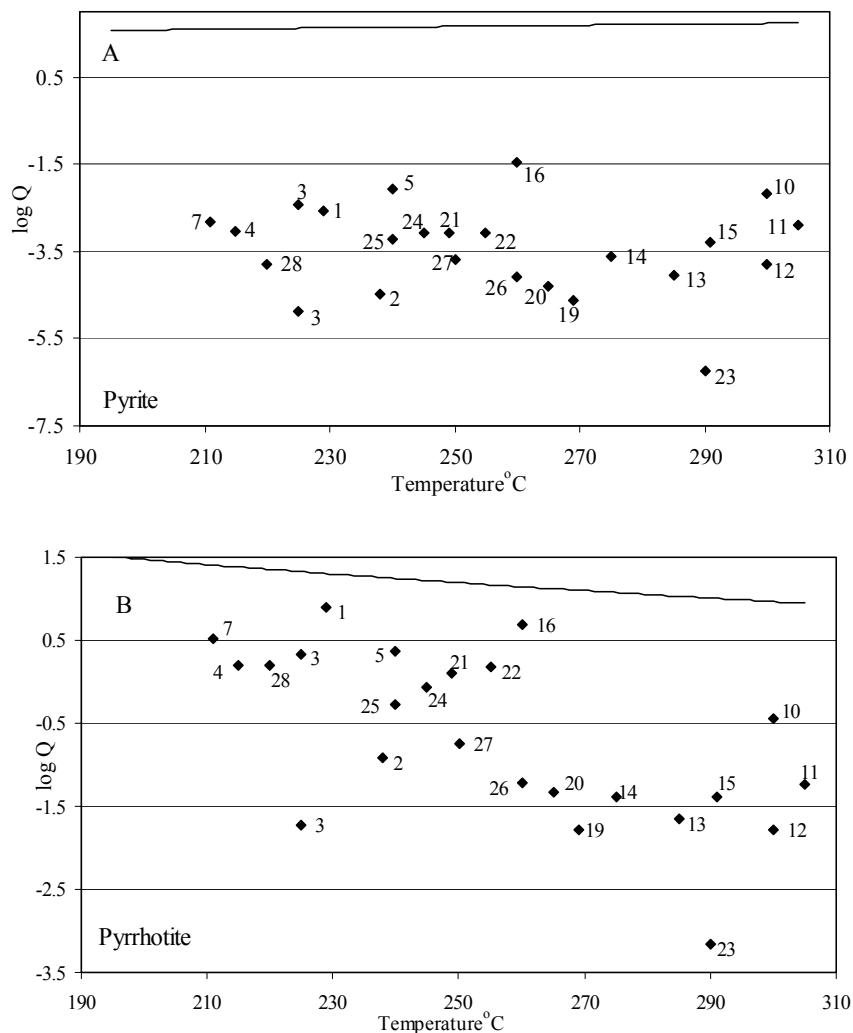


FIGURE 7: The saturation state of aquifer waters in selected geothermal systems with respect to pyrite and pyrrhotite; the solid curves represent the solubility constant values (log K) for each mineral and the numbers refer to the first column of Table 1

as hydrothermal minerals in many of the areas considered for the present study. They have precipitated from the water, and the water cannot, therefore, be undersaturated with them. The apparent strong undersaturation is most likely the result of faulty thermodynamic data on Fe-hydrolysis constants leading to low values for the calculated activity of the Fe^{+2} ion by the WATCH program (Gudmundsson and Arnórsson, 2001).

5.7 Prehnite

The solubility product for prehnite, which has been plotted in Figure 8A, shows considerable scatter. All the Zunil wells (ZCQ-3, 4, 5, 6), and most of the Icelandic wells, except for NG-6 and NJ-13, are oversaturated with respect to prehnite. On the other hand, most of the Olkaria wells, except OW-10, and the Nicaragua wells, except for MT-26, are undersaturated and all the Kizildere waters are strongly undersaturated, by 4-7 orders of magnitude. The average and mean departures from equilibrium are -0.603 and 1.787 log(Q/K) units, respectively and the standard deviation is 2.341. There are two calcium atoms per formula unit in prehnite so departure from equilibrium per calcium is 2-3.5 orders of magnitude, or considerably higher than that for calcite. Therefore, the observed undersaturation cannot be explained by loss of calcium from solution by calcite precipitation. The results are taken to indicate that prehnite is not stable in the Kizildere aquifers.

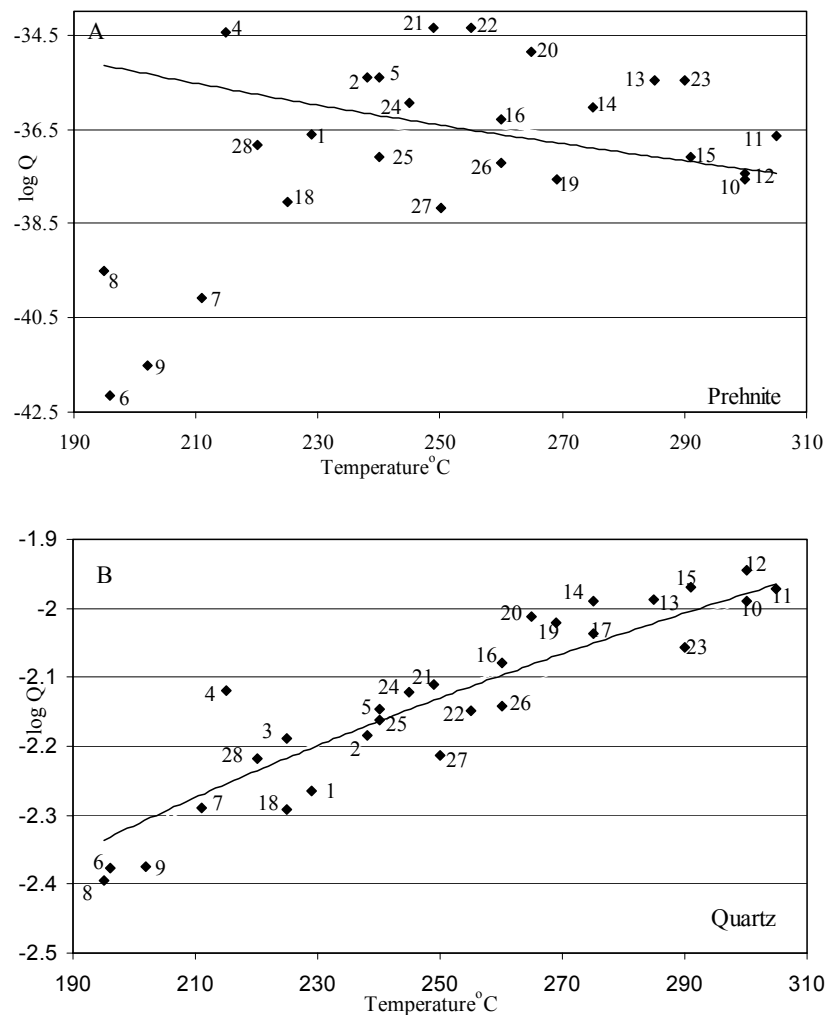


FIGURE 8: The saturation state of aquifer waters in selected geothermal systems with respect to prehnite and quartz; the solid curves represent the solubility constant values (log K) for each mineral and the numbers refer to the first column of Table 1

5.8 Quartz

Probably one of the most extensively studied mineral-solution equilibria in geothermal systems involves quartz. It has been well established that water in geothermal aquifers closely approaches equilibrium with quartz, at least when above 180°C (Arnórsson, 1975). Indeed the results shown in Figure 8B conform with this. The average and mean departures are 0 (no departure) and 0.039 log(Q/K) units, respectively (Table 2). The only aquifer water, which is heavily oversaturated, is that of Krafla well K-9. This may be an artifact. There is considerable discrepancy between the solute geothermometer (SiO₂, Na/K and Na-K-Ca) temperatures, the quartz geothermometer giving the highest value. The selected aquifer temperature of 215°C is the average of the mentioned solute geothermometers.

5.9 Wollastonite

The results depicted in Figure 9 for wollastonite show mostly slightly negative log(Q/K) values. The average and mean departure from equilibrium corresponds to -0.819 and 0.999 log(Q/K) units, respectively. Waters from wells K-9, NJ-16, ZCQ-3, 4 and 6, and MT-26 are close to saturation. The Kizildere wells again show strong undersaturation, the reason being low calcium in the discharge compared to the aquifer water due to calcite deposition as explained above. Excluding the Kizildere wells yields average and mean departures from equilibrium of -0.342 and 0.482 log(Q/K) units, respectively.

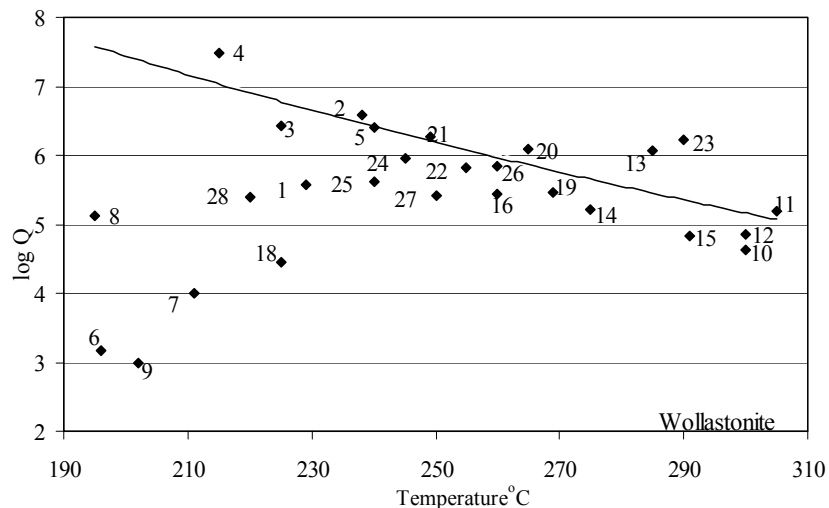


FIGURE 9: The saturation state of aquifer waters in selected geothermal systems with respect to wollastonite; the solid curves represent the solubility constant values (log K) for each mineral and the numbers refer to the first column of Table 1

5.10 Cation/Proton activity ratios

At overall mineral-solution equilibrium in geothermal systems hosted in basaltic to silicic volcanics, it has been shown that all major element cation/proton activity ratios attain a particular value at a specific temperature (Arnórsson et al., 1983a). Arnórsson et al. (1983a) provide temperature equations which describe cation/proton ratios at equilibrium. In rocks which differ much in composition from basaltic to silicic volcanics, these ratios may differ at equilibrium because different minerals are involved. In view of these observations, it is useful to study cation/proton activity ratios in the aquifer water of geothermal systems. Departure from the anticipated equilibrium value may be due to analytical imprecision, differences between aqueous cation concentrations in wellhead samples and aquifer fluid, faulty values for the computed aquifer water pH, lack of mineral-solution equilibrium, or equilibration with hydrothermal minerals other than those forming in volcanic rocks. The systematics in departure from equilibrium for different cation/proton activity ratios may help in identifying which species activity carries a faulty value.

The cation/proton activity ratios of the samples considered for the present study have been plotted in Figures 10-12. Al was not plotted as the activity ratio of $\text{Al}^{+3}/(\text{H}^+)^3$ but as $\text{Al}(\text{OH})_4^-/\text{OH}^-$ (see Arnórsson et al., 1983a). Na/H and K/H activity ratios plot on both sides of the equilibrium curve, the average and mean departure from the curves being 0.389, 0.307 and 0.359, 0.290 log(Q/K) units, respectively. The same pattern is observed for both ratios reflecting that Na/K ratios show much less scatter than the Na/H and K/H ratios. This suggests that the scatter of the data points in Figure 10 is mostly due to error in the calculated aquifer water pH. This is substantiated by the results for the Ca/H and Mg/H ratios. However, the Kizildere water shows low calcium/proton ratios in relation to both Na/H and K/H activity ratios, which is explained by loss of calcium from the solution from the Kizildere water as it boils and precipitates calcite.

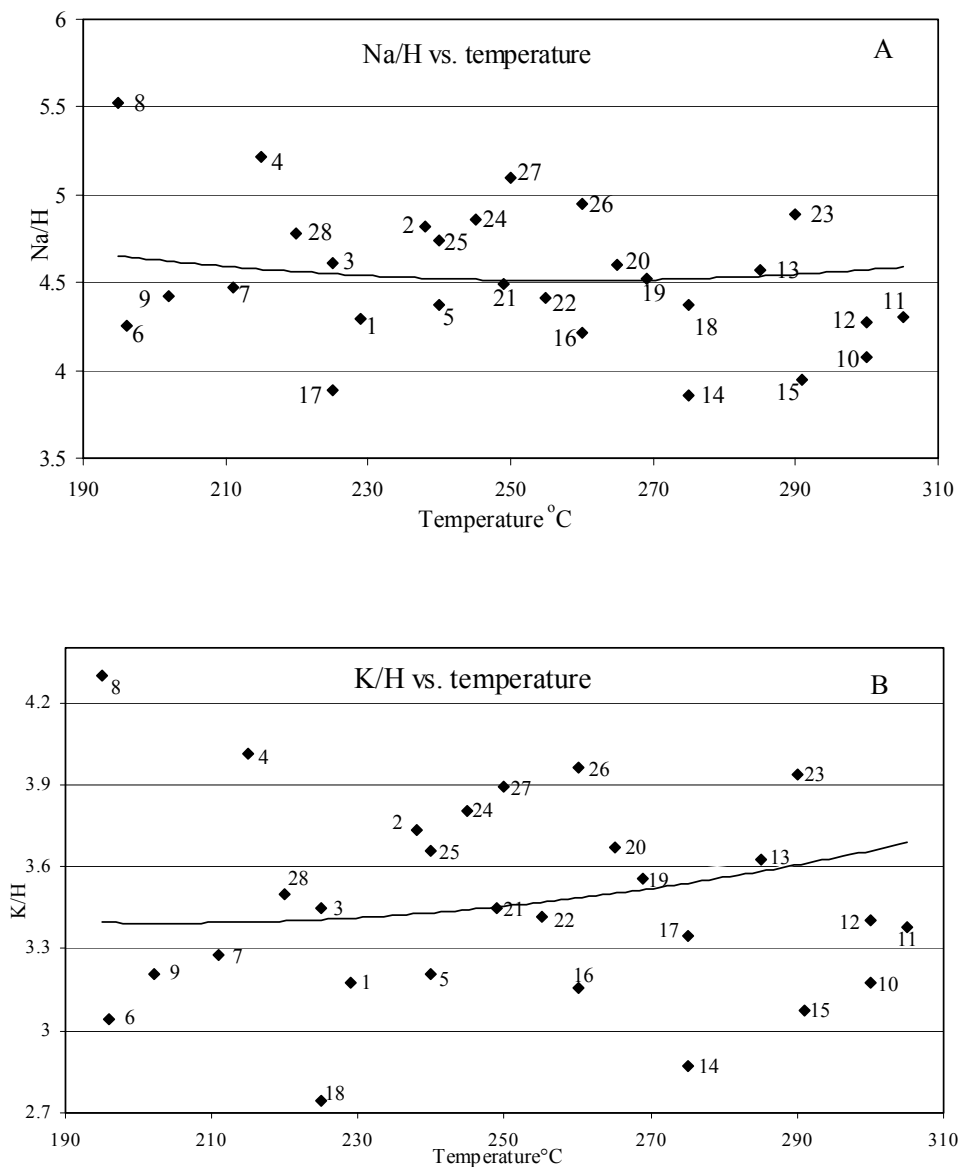


FIGURE 10: Variations of Na/H and K/H activity ratios in selected aquifer waters; solid curves show activity ratios at equilibrium temperature (equations taken from Arnórsson et al. (1983a)) and numbers refer to the first column of Table 1

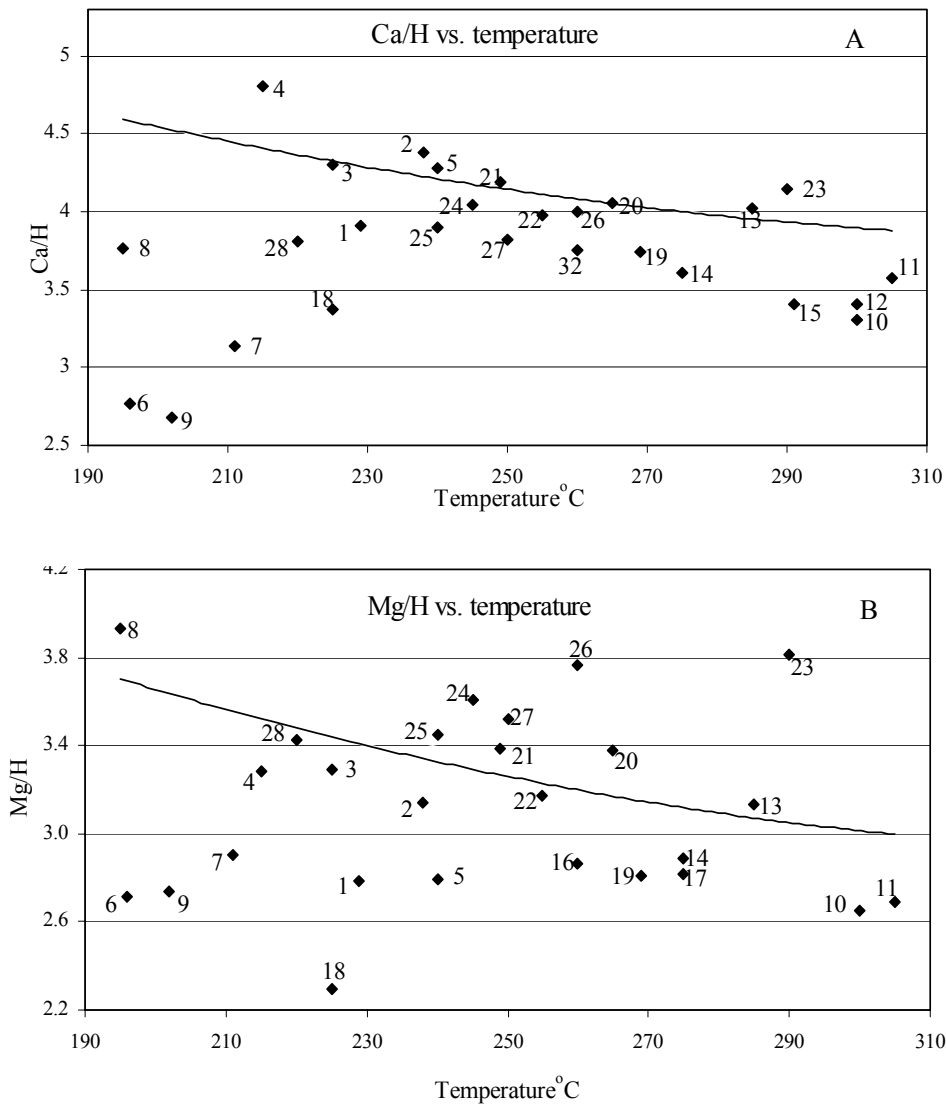


FIGURE 11: Variations of $Ca^{0.5}/H$ and $Mg^{0.5}/H$ activity ratios in selected aquifer waters; solid curves show activity ratios at equilibrium temperature (equations taken from Arnórsson et al. (1983a)) and numbers refer to the first column of Table 1

6. SCALING

6.1 General

Scale formation from geothermal waters is frequently encountered both in wells and surface equipment. Prediction of the scaling potential from geothermal waters is important for evaluation of the production characteristics of geothermal reservoirs and for taking necessary actions to prevent or control scale formation. Assessment of scaling potential involves assessment of the saturation state of the scale forming minerals. The minerals which are known to form scales include calcite (and aragonite), anhydrite, amorphous silica, poorly crystalline or amorphous Mg-silicate, Al-silicate and sulphides of iron and other metals. Many minerals found as hydrothermal minerals in geothermal systems are not known to form scales in wellbores although the water becomes oversaturated with respect to these minerals as a consequence of boiling and cooling. The reason must be sluggish kinetics.

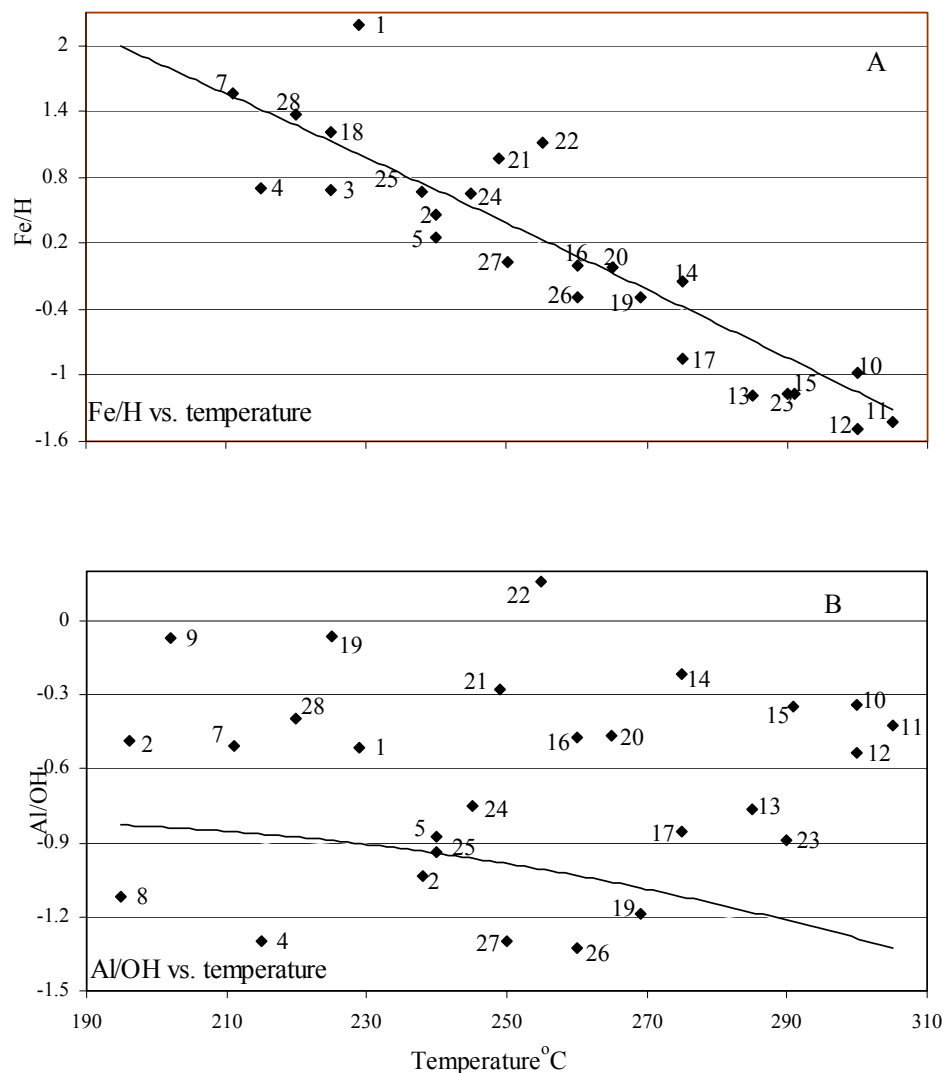


FIGURE 12: Variations of $\text{Fe}^{0.5}/\text{H}$ and Al/OH activity ratios in selected aquifer waters; solid curves show activity ratios at equilibrium temperature (equations taken from Arnórsson et al. (1983a)) and numbers refer to the first column of Table 1

Operational problems associated with scale formation include reduced fluid flow preventing valves from closing and scaling of turbine blades. The most troublesome scales involve calcite and amorphous silica (Arnórsson, 1989; Ármannsson, 1989; Kristmannsdóttir, 1989; Líndal and Kristmannsdóttir, 1989). The discussion below is confined to these types of scales.

In wet-steam wells, calcite scaling has only been troublesome when the level of first boiling is in the well. Precipitation begins at this level where it is also most intense. At higher levels, it decreases and may disappear altogether below the wellhead or still be intense at the surface. Geothermal aquifer water is always close to calcite saturation. Boiling causes a drastic decrease in CO_2 partial pressures, which leads to calcite oversaturation and precipitation. The oversaturation reaches maximum at a temperature which is a few tens of degrees lower than the temperature at which boiling sets in. At this maximum, the water has been almost quantitatively degassed. Further boiling, which leads to cooling, will successively cause less oversaturation as the solubility of calcite increases with decreasing temperature. The intensity of calcite precipitation relates to the aquifer temperature, the calcium concentration in the water, and CO_2 partial pressure. Problems caused by calcite scaling in wet-steam wells can be solved by using chemical inhibitors, or mechanically by periodic cleaning of the wells. The selection of methods for solving scaling problems needs to consider both technical and economic aspects. Calcite scaling may occur from waste water from geothermal power plants, especially when injected into deep wells that penetrate hot aquifers.

In geothermal aquifers, silica concentrations are controlled by quartz solubility. Cooling by boiling, accompanied by an increase in aqueous silica concentrations by steam loss, cause the water to become quartz oversaturated. However, quartz precipitation is sluggish, and silica is only removed from solution at an appreciable rate if the solution becomes somewhat oversaturated with amorphous silica, particularly when this oversaturated water comes into contact with air. Troublesome scaling of silica is sometimes encountered in waste water discharged to the atmosphere in high-temperature fields. The temperature at which amorphous silica saturation is reached in wet-steam well water, depends on the aquifer temperature, the change in pH of the water as it boils and possible separation of the water and steam phases in the aquifer flowing towards the well (Arnórsson, 1989). Ionization of dissolved silica, caused by pH increase, lowers the temperature at which amorphous silica saturation is reached. The rate of amorphous silica precipitation is positively related to water temperature, the degree of water oversaturation and water salinity, but negatively related to the extent of polymerization of dissolved silica. The effects of temperature and water salinity dominate. Precipitation of ferric iron, produced by oxidation of ferrous iron when geothermal water comes into contact with the air, may catalyze the precipitation of amorphous silica. It is observed that silica scales form most rapidly from very hot and saline brines, which are high in iron, and precipitate appreciable quantities of iron sulphides.

6.2 Calcite scaling tendencies in production wells

In order to demonstrate calcite-scaling tendencies in production and injection wells, chemical data from three wells used in the present study were selected (Kizildere, well KD-16; Zunil, well ZCQ-5 and Nesjavellir, well NJ-11). Figure 13 shows the calculated state of calcite saturation for the waters in these three wells during single step adiabatic boiling, assuming degassing to be at maximum, i.e. equilibrium distribution is attained for all gases present between the water and steam phases. All the selected waters show a change towards calcite oversaturation during the early stages of boiling. It is most pronounced for the relatively cool Kizildere well but minor for the hottest Nesjavellir well. These results reflect the temperature dependence of CO₂ solubility. The solubility of this gas in the water is considerably higher at the aquifer temperature of the hottest well considered (305°C) as compared to that of the coldest well (211°C). Thus, degassing becomes more effective at lower water temperature and more degassing brings about more of an increase in the value taken by the calcite saturation index. For the Zunil and Nesjavellir wells, calcite over-saturation reaches a maximum at some 20°C below the aquifer temperature. Below this, maximum oversaturation decreases and eventually waters from both wells become calcite undersaturated. Around the maximum, the waters from the Zunil and Nesjavellir wells have been almost completely degassed, so further cooling by boiling leads to progressively lower calcite saturation index values due to the retrograde solubility of calcite. For the Kizildere well calcite oversaturation is

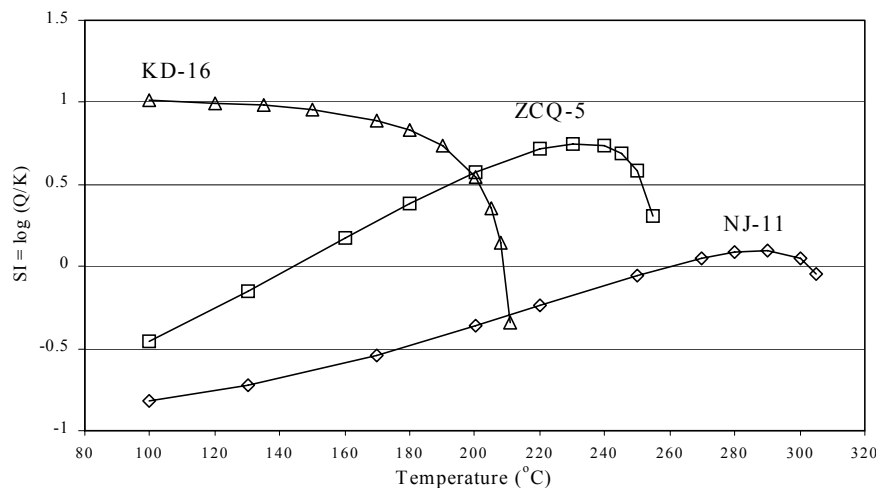


FIGURE 13: Changes in the state of the calcite saturation in waters from wells KD-16 (Kizildere), ZQ-5 (Zunil) and NJ-11 (Nesjavellir) upon adiabatic boiling

maintained at low temperature. The relatively gas rich water from this well is not completely degassed, even at 100°C. An increasing degree of calcite oversaturation during the early stages of boiling of the water in this well occurs because the degassing effect dominates the effect of retrograde calcite solubility. At lower temperatures, the relative effect of retrograde calcite solubility becomes more important.

6.3 Amorphous silica scaling tendencies in production wells

Figure 14 shows the calculated state of amorphous silica saturation for waters from the wells discussed in the previous section. The cooling, which results from boiling, causes the water to become oversaturated with respect to amorphous quartz because its solubility decreases with decreasing temperature. For the KD-6 well, amorphous silica saturation is not reached until at $\sim 80^\circ\text{C}$. ZCQ-5 and NJ-11 well waters reach saturation at $\sim 135^\circ\text{C}$ and $\sim 190^\circ\text{C}$, respectively (Figure 14). In order to avoid amorphous silica scaling in wells NJ-11 and ZCQ-5, wellhead pressure should be maintained above about 12 and 4 bar-a, respectively. In contrast, it is safe to flash the Kizildere KD-16 well water to atmospheric pressure.

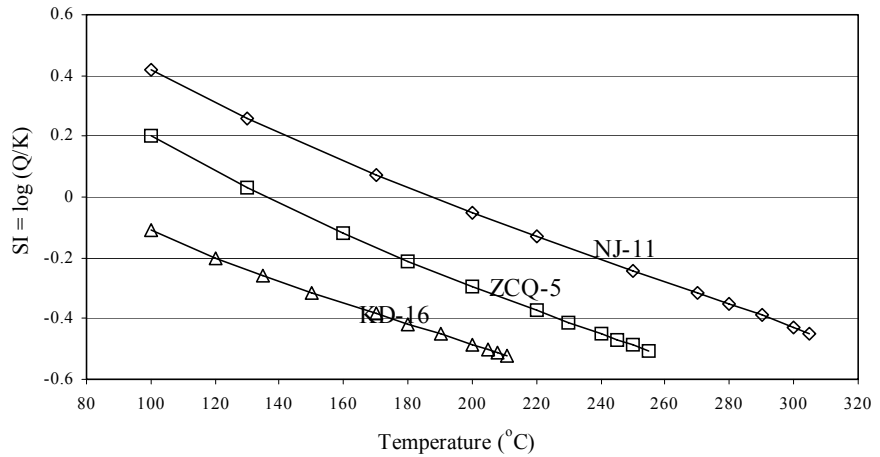


FIGURE 14: Changes in the state of amorphous silica saturation in waters from wells KD-16 (Kizildere), ZCQ-5 (Zunil) and NJ-11 (Nesjavellir) upon adiabatic boiling

6.4 Calcite and amorphous quartz scaling tendencies in reinjection wells

It is an important practice to dispose of waste geothermal fluid by injection, either into shallow or deep drillholes. Such drillholes may be located within production well fields or outside them, even outside the geothermal area. If the water is disposed of by injection into shallow drillholes, it may be expected to cool further. On the other hand, if injected into deep wells, it may gain heat. The temperature changes may bring about oversaturation with respect to some minerals, thus creating a tendency for them to deposit from the water. It is important to assess the state of mineral saturation in waste geothermal fluid that is intended to be disposed of by injection in order to find out the optimum temperature for injection (Arnórsson et al., 2000).

Figure 15 shows the calculated state of calcite saturation of the waters from the three selected wells, associated with conductive cooling and heating subsequent to flashing to atmospheric pressure (100°C). The Zunil and the Nesjavellir well waters attain saturation upon heating to 160°C and 190°C , respectively, and with increasing temperature they become progressively more oversaturated. The Kizildere

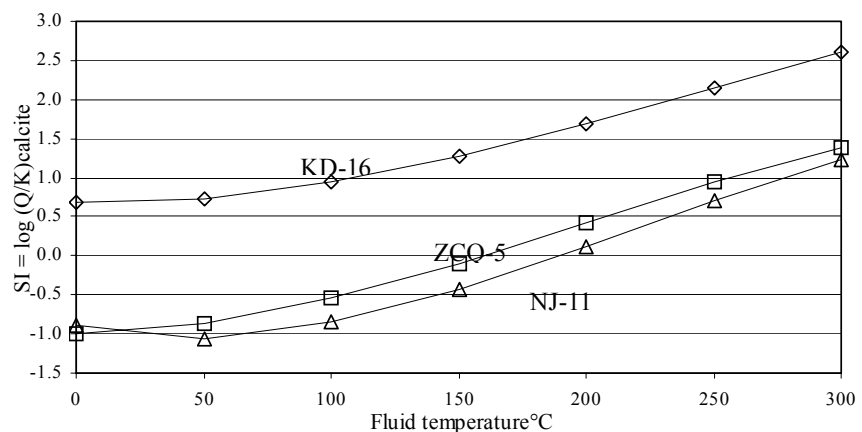


FIGURE 15: Changes in the state of calcite saturation in waters from wells KD-16 (Kizildere), ZCQ-5 (Zunil) and NJ-11 (Nesjavellir) upon conductive cooling

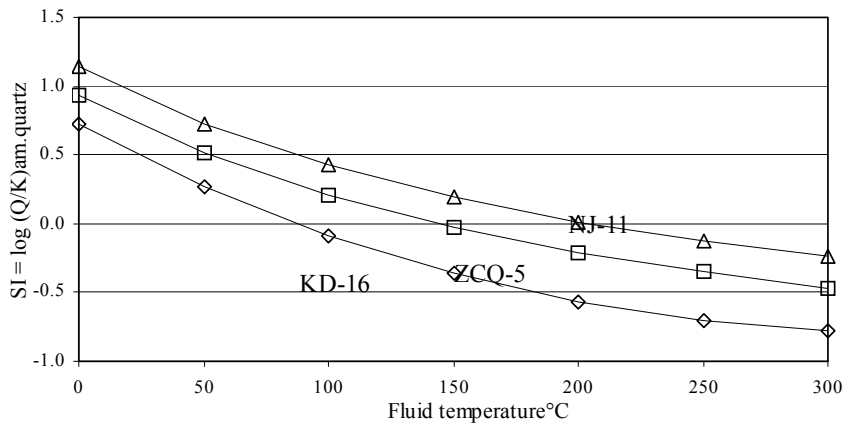


FIGURE 16: Changes in the state of amorphous silica saturation in waters from wells KD-16 (Kizildere), ZCQ-5 (Zunil) and NJ-11 (Nesjavellir) upon conductive cooling

KD-6 well water is calcite oversaturated at all temperatures and the degree of oversaturation increases with rising temperature, particularly above about 100°C.

The state of amorphous silica saturation for the same wells is shown in Figure 16. The Kizildere well water is oversaturated below 80°C but undersaturated at higher temperatures. The same values for wells ZCQ-5 and NJ-11 are 150 and 210°C, respectively.

Combining the results for calcite and amorphous silica saturation states show that the Kizildere water is oversaturated with one or both minerals at all temperatures. In the range 150-160°C, the Zunil well water is undersaturated with both calcite and amorphous silica and the Nesjavellir water around 200°C. Optimum injection temperatures for the Zunil and Nesjavellir waters are, accordingly, about 150°C and 200°C, respectively. It is considered most feasible to inject the Kizildere water at the lowest temperature possible. Under these conditions, calcite oversaturation is minimal and experience has shown that amorphous silica deposition, even from highly oversaturated solution, is very sluggish below about 50°C.

7. SUMMARY AND CONCLUSIONS

The present study describes the state of mineral saturation in high-temperature geothermal aquifers from selected areas. The areas include Krafla, Námafjall, Nesjavellir and Hveragerdi in Iceland, Olkaria in Kenya, Zunil in Guatemala, Momotombo in Nicaragua and finally Kizildere in Turkey. The recorded aquifer temperatures of the selected areas are between 195 and 305°C. Most of the selected wells for this study have excess enthalpy (the discharge enthalpy is higher than that of liquid water at aquifer temperature), but some of them have liquid enthalpy (the discharge enthalpy is equal to that of steam saturated water at aquifer temperature). The aquifer water composition and speciation distribution were calculated with the aid of WATCH program. For these calculations, the total discharge composition of the liquid enthalpy wells was taken to represent the aquifer water composition. For the excess enthalpy wells, on the other hand, it was assumed that the excess enthalpy was due to segregation of the flowing water and steam in the aquifer (thermodynamically open system).

The hydrothermal minerals considered are anhydrite, calcite, clinocllore, daphnite, clinzoisite, epidote, grossular, wairakite, low-albite, microcline, pyrite, pyrrhotite, prehnite, quartz and wollastonite. The aquifer waters depart insignificantly from saturation with quartz. They are also very close to saturation with respect to calcite, low-albite and microcline. However, the results for the Kizildere water indicate significant undersaturation. This is an artifact due to low calcium in the well discharges as compared to those in the aquifer water, the consequence of extensive calcite precipitation as the water boils. When incorporating the Al-Si dimer into the speciation calculations, the results indicate slight yet systematic undersaturation of the alkali feldspars. If, on the other hand, the dimer is omitted slight systematic oversaturation is indicated. These results are consistent with those of Stefánsson and Arnórsson (2000). A possible cause is overestimation of the stability of the Al-Si dimer. The results for other minerals show more scatter, in particular the OH-bearing Al-silicates, which have a relatively complex composition. The same applies for pyrite and pyrrhotite.

The more saline waters (Momotombo, Zunil) tend to be close to anhydrite saturation whereas the more dilute waters (other areas) are undersaturated. Systematic oversaturation is observed for the clinocllore component of chlorite, but systematic undersaturation for the daphnite component. On the other hand, the data points for the clinozoisite component of epidote scatter around the equilibrium curve, but systematic strong oversaturation is observed for the epidote component. This apparent oversaturation is probably the consequence of faulty thermodynamic data on epidote. As for clinozoisite, the data points for wairakite and grossular scatter around equilibrium. Some waters are close to wollastonite saturation, others are undersaturated.

A noteworthy result is that the Kizildere water is systematically undersaturated with all calcium-bearing minerals. This is certainly, in part, an artifact, due to the removal of calcium from solution by extensive calcite precipitation. However, such precipitation does not explain the observed degree of undersaturation. The Kizildere aquifer water is relatively cool and some of the Ca-bearing minerals considered for the present study such as prehnite and clinozoisite-epidote, may not be stable at these low temperatures.

Imprecise thermodynamic data on iron hydrolysis constants probably leads to low values for the calculated activities of the Fe^{+2} species, leading to low values for $\log Q$ for all ferrous bearing minerals (daphnite, pyrite and pyrrhotite) and, thus, strong apparent undersaturation.

The observed scatter of Na/H, K/H, Ca/H, Mg/H, Fe/H and Al/H ion activity ratios is mostly the consequence of error in the calculated aquifer water pH. However, some waters, in particular Kizildere waters, display low Ca/H ion activity ratios in relation to both Na/H and K/H ion activity ratios. This is explained by a loss of calcium from solution as calcite precipitates during boiling.

Calcite and amorphous silica scaling potentials were assessed for three of the well discharges considered in the present study (Nesjavellir NJ-11, Zunil ZCQ-5 and Kizildere KD-16). The assessment included scaling potentials as the water boils (production wells), but also through temperature changes of water which had previously flashed to 100°C. The results indicate that calcite-scaling potential only exists over a limited temperature range after boiling sets in, whereas the Kizildere water maintains heavy oversaturation from the onset of boiling to low temperatures. Onset of potential deposition of amorphous silica is positively related to aquifer temperature, being 190°C for the hottest well (Nesjavellir) and less than 100°C for the coolest well (Kizildere). The results indicate that cold injection is favourable for Kizildere if calcite and amorphous silica deposition is to be avoided in injection wells. Hot injection is, on the other hand favourable for Zunil (around 150°C) and Nesjavellir (180-260°C).

ACKNOWLEDGEMENTS

Special thanks to my supervisor, Professor Stefán Arnórsson, who suggested and guided this study, and also provided the data. I am honoured to have been his student. I would like to express my sincere gratitude to the UNU staff, Director Dr. Ingvar B. Fridleifsson, Deputy Director Mr. Lúdvík S. Georgsson and Mrs. Gudrún Bjarnadóttir Administrative Assistant for all the care, generous help and advice, during the whole training period. Finally, my deepest thanks to my wife Gonca, and children Berilsu and Deniz for their moral support during the six-months I was away from home.

REFERENCES

- Ármansson, H., 1989: Predicting calcite deposition in Krafla boreholes. *Geothermics*, 18, 25-32.
- Ármansson, H., Benjamínsson, J., and Jeffrey, A.W.A., 1989: Gas changes in the Krafla geothermal system, Iceland. *Chemical Geology*, 76, 175-196.
- Ármansson, H., Gudmundsson, Á., and Steingrímsson, B.S., 1987: Exploration and development of the Krafla geothermal area. *Jökull*, 37, 12-29.
- Arnórsson, S., 1975: Application of the silica geothermometer in low-temperature hydrothermal areas in Iceland. *Am. J. Sci.*, 275, 763-783.
- Arnórsson, S., 1989: Deposition of calcium carbonate minerals from geothermal waters-theoretical considerations. *Geothermics*, 18, 33-39.
- Arnórsson, S., 1995: *Geochemical investigations of geothermal resources in Guatemala*. IAEA, project no. GUA/8/009-06, report, Vienna.
- Arnórsson, S., 1997: *Interpretation of chemical and isotopic data on fluids discharged from wells in the Momotombo geothermal field, Nicaragua*. Report on an expert mission to Nicaragua January 19th to February 1st 1997.
- Arnórsson, S., 1999: The relative abundance of Al-species in natural waters in Iceland. *Proceedings of the 5th International Symposium on the Geochemistry of the Earth's Surface*, Balkema, Rotterdam, 421-424.
- Arnórsson, S., 2000a: The quartz and Na/K geothermometers. I. New thermodynamic calibration. *Proceedings of the World Geothermal Congress 2000, Kyushu-Tohoku, Japan*, 929-934.
- Arnórsson, S., 2000b: The quartz and Na/K geothermometers. II. Results and application for monitoring studies. *Proceedings of the World Geothermal Congress 2000, Kyushu-Tohoku, Japan*, 935-940.
- Arnórsson, S., and Andrésdóttir, A., 1999: The dissociation constants of Al-hydroxy complexes at 0-350 °C and P_{sat} . *Proceedings of the 5th International Symposium on the Geochemistry of the Earth's Surface*, Balkema, Rotterdam, 425-428.
- Arnórsson, S., Björnsson, S., Muna, Z.W., and Bwire-Ojiambo, S., 1990: The use of gas chemistry to evaluate boiling processes and initial steam fractions in geothermal reservoirs with an example from the Olkaria field, Kenya. *Geothermics* 19, 497-514.
- Arnórsson, S., D'Amore, F., and Gerardo-Abaya, J., 2000: *Isotopic and chemical techniques in geothermal exploration, development and use*. IAEA, Vienna, 351pp.
- Arnórsson, S., Geirsson, K., Andrésdóttir, A., and Sigurdsson, S., 1996: *Compilation and evaluation of thermodynamic data on aqueous species and dissociational equilibria in aqueous solutions. I. The solubilities of CO₂, H₂S, H₂, CH₄, N₂, O₂ and Ar in pure water*. University of Iceland, Science Institute, report RH-17-96, 20 pp.
- Arnórsson, S., Gunnlaugsson, E., and Svavarsson, H., 1983a: The chemistry of geothermal waters in Iceland II. Mineral equilibria and independent variables controlling water compositions. *Geochim. Cosmochim. Acta*, 47, 547-566.

Arnórsson, S., Gunnlaugsson, E., and Svavarsson, H., 1983b: The chemistry of geothermal waters in Iceland III. Chemical geothermometry in geothermal investigations. *Geochim. Cosmochim. Acta*, 47, 567-577.

Arnórsson, S., Sigurdsson, S., and Svavarsson, H., 1982: The chemistry of geothermal waters in Iceland I. Calculation of aqueous speciation from 0°C to 370°C. *Geochim. Cosmochim. Acta*, 46, 1513-1532.

Arnórsson, S., Stefánsson, A., Gunnarsson, I., Andrésdóttir, A., and Sveinbjörnsdóttir, A.E., 2001: Major element chemistry of surface and ground waters in basaltic terrain, N- Iceland. I. Primary mineral saturation. *Geochim. Cosmochim. Acta*, (in press).

Bjarnason, J.Ö., 1994: *The speciation program WATCH, version 2.1*. Orkustofnun, Reykjavík, 7 pp.

Combredet, N., Guilhaumou, N., Cormy, G., and Tiffer, E.M., 1987: Petrographic correlations and analysis of fluid inclusions in hydrothermal quartz crystals from four wells in the Momotombo geothermal field, Nicaragua. *Geothermics*, 16, 239-254.

Diakonov, I.I., Schott, J., Martin, F., Harrichourry, J.C., and Escalier, J., 1999: Iron (III) solubility and speciation in aqueous solutions. Experimental study and modeling: part 1. Hematite solubility from 60 to 300°C in NaOH-NaCl solutions and thermodynamic properties of $\text{Fe}(\text{OH})_{4(\text{aq})}$. *Geochim. Cosmochim. Acta*, 63, 2247-2261.

ENEL, 1989: *Optimization and development of the Kizildere geothermal field*. ENEL, Aquater, DAL and Geotermica Italiana, Pisa, Italy, final report.

Franzson, H., 2000: Hydrothermal evolution of the Nesjavellir high-temperature system, Iceland. *Proceedings of the World Geothermal Congress 2000, Kyushu-Tohoku, Japan*, 2075-2080.

Giese, L.B., 1997: *Geotechnische und umwelt geologische aspekte bei der forderung und reinjection von thermal fluiden zur nutzung geothermischer energie am beispiel des geothermal feldes Kizildere und des umfeldes, W-Anatolien/Turkei (in German)*. University of Berlin, Ph.D. thesis, 201 pp.

Giggenbach, W.F., 1980: Geothermal gas equilibria. *Geochim. Cosmochim. Acta*, 44, 2021-2032.

Giggenbach, W.F., 1981: Geothermal mineral equilibria. *Geochim. Cosmochim. Acta*, 45, 393-410.

Giggenbach, W.F., 1988: Geothermal solute equilibria. Derivation of Na-K-Mg-Ca geothermometers. *Geochim. Cosmochim. Acta*, 52, 2749-2765.

Gökgöz, A., 1998: Geochemistry of the Kizildere-Tekkehamam-Buldan-Pamukkale geothermal fields, Turkey. Report 5 in: *Geothermal training in Iceland 1998*. UNU G.T.P., 115-156.

Gudmundsson, B.T., and Arnórsson, S., 2001: Secondary mineral-fluid equilibria in the Krafla and Námafjall geothermal systems, Iceland. *Applied Geochemistry*, (in press).

Gunnarsson, I., and Arnórsson, S., 1999: Amorphous silica solubility and the thermodynamic properties of H_4SiO_4 in the range 0° to 350°C at Psat. *Geochim. Cosmochim. Acta*, 64, 2295-2307.

Karingithi, C.W., 2000: Geochemical characteristics of the Greater Olkaria geothermal field, Kenya. Report 9 in: *Geothermal training in Iceland 1998*. UNU G.T.P., 165-188.

Kristmannsdóttir, H., 1989: Types of scaling occurring by geothermal utilization in Iceland. *Geothermics*, 18, 183-190.

- Labota, E.M., and Palma, J., 2000: The Zunil-II geothermal field, Guatemala, Central America. *Proceedings of the World Geothermal Congress 2000, Kyushu-Tohoku, Japan*, 2133-2138.
- Líndal, B., and Kristmannsdóttir, H., 1989: The scaling properties of the effluent water from Kizildere power station, Turkey, and recommendation for a pilot plant in view of district heating applications. *Geothermics*, 18, 217-223.
- Michard, G., 1991: The physical chemistry of geothermal systems, In D'Amore, F. (coordinator), *Application of geochemistry in geothermal reservoir development*. UNITAR/UNDP publication, Rome, 197-214.
- Muchemi, G.G., 1999: *Conceptualised model of the Olkaria Geothermal Field*. The Kenya Electricity Generating Company, Ltd, internal report, 46 pp.
- Nielsen, G., Maack, R., Gudmundsson, A., and Gunnarsson, G.I., 2000: Completion of Krafla geothermal power plant. *Proceedings of the World Geothermal Congress 2000, Kyushu-Tohoku, Japan*, 3259-3264.
- Omenda, P.A., 1998: The geology and structural controls of the Olkaria geothermal system, Kenya. *Geothermics*, 27-1, 55-74.
- Palandri, J.L., and Reed, M.H., 2001: Reconstruction of in situ composition of sedimentary formation waters. *Geochim. Cosmochim. Acta*, 65, 1741-1767.
- Pokrovskii, G.S., Schott, J., Salvi, S., Gout, R., and Kubicki, J.D., 1998: Structure and stability of aluminium-silica complexes in neutral to basic solution. Experimental study and molecular orbital calculations. *Mineralogical Magazine*, 62A, 1194-1195.
- Simsek, S., 1985: Geothermal model of Denizli-Saraykoy-Buldan area. *Geothermics*, 14, 393-417.
- Stefánsson, A., and Arnórsson, S., 2000: Feldspar saturation state in natural waters. *Geochim. Cosmochim. Acta*, 64, 2567-2584.
- Stefánsson, A., Gíslason, S.R., and Arnórsson, S., 2000: Dissolution of primary minerals in natural waters II. Mineral saturation state. *Chemical Geology*, 172, 251-276.
- Tole, M.P., Ármannsson, H., Pang Z.H., and Arnórsson, S., 1993: Fluid/mineral equilibrium calculations for geothermal fluids and chemical geothermometry. *Geothermics*, 22, 17-37.